

Molecular dynamics simulation study of the high frequency sound waves in the fragile glass former ortho-terphenyl.

S. Mossa^{1,2}, G. Monaco³, G. Ruocco², M. Sampoli⁴, and F. Sette³

¹ Center for Polymer studies and Department of Physics, Boston University, Boston, Massachusetts 02215.

² Dipartimento di Fisica and INFM, Università di Roma "La Sapienza" P.zza Aldo Moro 2, Roma, I-00185, Italy

³ European Synchrotron Radiation Facility, BP220, Grenoble Cedex, F-38043, France

⁴ Dipartimento di Energetica and INFM, Università di Firenze, Via Santa Marta 3, Firenze, I-50139, Italy

(November 5, 2018)

Using a realistic flexible molecule model of the fragile glass former orthoterphenyl, we calculate via molecular dynamics simulation the collective dynamic structure factor $S(Q, \omega)$, recently measured in this system by Inelastic X-ray Scattering. The comparison of the simulated and measured dynamic structure factor, and the study of the $S(Q, \omega)$ in an extended momentum (Q), frequency (ω) and temperature range allows: *i*) to conclude that the utilized molecular model gives rise to $S(Q, \omega)$ in agreement with the experimental data, for those thermodynamic states and Q values where the latter are available; *ii*) to confirm the existence of a slope discontinuity on the T dependence of the sound velocity that, at finite Q 's, takes place at a temperature T_x higher than the calorimetric glass transition temperature T_g ; *iii*) to find that the values of T_x is Q -dependent and that its $Q \rightarrow 0$ limit is consistent with T_g . The latter finding is interpreted within the framework of the current description of the dynamics of supercooled liquids in terms of exploration of the potential energy landscape.

PACS numbers: 64.70.Pf, 71.15.Pd, 61.25.Em, 61.20.-p

I. INTRODUCTION

The understanding of the dynamics of the supercooled liquids [1,2] and of its relation with the glass transition has received great attention in the last few years. Different details of the dynamics of supercooled liquids and glasses seem to be on the way to be settled, while other are still obscure. As an example, considering the dynamics of the density fluctuations which are the main issue for this paper, on one side the connection between the glass transition phenomenology and the long time dynamics (*structural rearrangement*) has been almost clarified, on the other side the effect of the structural arrest on the high frequency collective vibrational motion (*sound waves*) is much less clear.

From the experimental point of view the study of the time behavior of the density fluctuations is made via the determination of the dynamic structure factor $S(Q, \omega)$, i. e. the power spectrum of the Q component of the number density $\rho_Q(t)$. In the hydrodynamic regime this quantity is measurable by laser light scattering, a well established technique ($Q \approx 0.03 \text{ nm}^{-1}$ corresponding to frequency in the GHz range). Thanks to this technique much is known about the collective dynamics in the nanosecond time scale. The limit of high frequencies (picosecond time scales) is traditionally the realm of the inelastic neutron scattering technique. This technique, however, suffers of strong kinematics limitations, that prevent the possibility to investigate the mesoscopic Q region ($Q \approx 1 \div 10 \text{ nm}^{-1}$) that is particularly interesting as it is the region where the transition from a gen-

uine collective behaviour of the density fluctuation fades in the single particle dynamics. Such kinematics limitations have been recently overcome by the Inelastic X-ray Scattering (IXS) technique. Using this techniques it has been possible to firmly establish few common features of the collective dynamics in glasses in the mesoscopic region [3]. In particular, beside from specific *quantitative* difference among different systems, all the investigated glasses show some *qualitative* common features that can be summarized as follows: *i*) there exist propagating acoustic-like excitations up to a max Q value (Q_m) given by $Q_m a \approx 1 \div 3$ showing up as more or less defined Brillouin peaks at $\Omega(Q)$ in the $S(Q, \omega)$ (here a is the average inter-particle distance). The specific value of $Q_m a$ result to be correlated with the fragility of the glass; *ii*) the slope of the (almost) linear $\Omega(Q)$ vs Q dispersion relation in the $Q \rightarrow 0$ limit extrapolates to the macroscopic sound velocity; *iii*) the broadening of the Brillouin peaks, $\Gamma(Q)$, follows a power law, $\Gamma(Q) = DQ^\alpha$, with $\alpha \approx 2$ within the statistical uncertainties; *iv*) the value of D does not depend significantly on temperature, indicating that the broadening (i.e. the sound attenuation) in the high frequency region does not have a dynamic origin, but rather that it is due to the topological disorder [4].

From a theoretical point of view, two main theories have been developed for the study of supercooled and glassy systems, one based on first principle computations of the equilibrium thermodynamics [5] and a second one, the Mode Coupling Theory (MCT) [6,7], dynamical in nature. Very recently they have been complemented with the interpretation of the thermodynamics and of the slow

structural dynamics in terms of the topological properties of the underlying Potential Energy Surface (PES) [8–10]. Such interpretation is based on the concept of *inherent structures*, introduced many years ago by Stillinger and Weber [11]: upon cooling, the system populates basins of the PES whose (local) minima have depth increasing on lowering the temperature. Moreover, in this framework, the dynamics of the systems has been thought to be decomposed in a “fast” -high frequency- vibrational dynamics describing the exploration of a specific basin and a “slow” -diffusive- one, associated to the exploration of different basins. In these studies a key role has been played by computer simulations that, considering the nowadays technology, permit a significant sampling of the PES also at low temperature and, in principle, the study of the dynamics of the model systems at every time scale.

Among other, one not yet fully explained issue in the high frequency collective dynamics of supercooled liquids and glasses is the recent findings that the temperature dependence of the excitations frequency at fixed Q value shows a slope discontinuity at a temperature, T_x , that is *larger* than the calorimetric glass transition temperature T_g [12,13]. This observation seems to connect to each other the shape of the PES basins (which determines the vibrational frequency and hence also the excitations frequency at a given Q 's) with the depth of the minima explored at that specific temperature. It is our aim to further investigate this issue.

In this paper we show results, obtained by means of molecular dynamics simulations, concerning the high frequency dynamics of a realistic *flexible* model [14–16] for the fragile glass former orthoterphenyl (OTP). Our aim is then twofold. First we want to study the capability of the utilized molecular model to reproduce the high frequency dynamics of OTP by comparing the calculated dynamics structure factor with the analogous experimental quantity. Once the model has been validate, our aim is i) to extend the experimental data to other Q 's and other thermodynamic points and ii) to provide an interpretation of the experimental finding of the existence of a slope discontinuity in the temperature dependence of the sound velocity [12,13].

The paper is organized as follows: in Sec. II we briefly describe the model and we define the dynamic structure factor $S(Q, \omega)$ that will be compared with the experimental results. In Sec. III we recall some of the theoretical model used in the analysis of the dynamic structure factor in liquids; we compare our results with the experimental sets of data [12,13] in a large temperature and momentum range finding a very good agreement; we discuss the connection between our findings and the PES approach to the dynamics. Finally in Sec. IV we discuss the results obtained and we draw some conclusions.

II. COMPUTATIONAL DETAILS

In our model [14] the OTP molecule is constituted by three rigid hexagons (phenyl rings) of side $L_a = 0.139$ nm. Two adjacent vertices of the *parent* (central) ring are bonded to one vertex of the two *side* rings by bonds whose length, at equilibrium, is $L_b = 0.15$ nm. In this scheme, each vertex of the hexagons is thought to be occupied by a fictitious atom of mass $M_{CH} = 13$ a.m.u. representing a carbon-hydrogen pair (C-H). In the isolated molecule, at equilibrium, the two lateral rings lie in planes that form an angle of about 54° with respect to the central ring's plane. The three rings of a given molecule interact among themselves by an *intra-molecular* interaction potential; such potential is chosen in such a way to give the correct relative equilibrium positions for the three phenyl rings, to preserve the molecule from “dissociation”, and to represent at best the isolated molecule vibrational spectrum. The interaction among the rings pertaining to different molecules is described by a site-site pairwise additive Lennard-Jones 6-12 potential, each site corresponding to one of the six hexagons vertices. The details of the intra-molecular and inter-molecular interaction potentials, together with the values of the involved constants, are reported in Ref. [14]. Previous studies of the temperature dependence of the self diffusion coefficient [14] and of the structural (α) relaxation times [14,15] indicate that the introduced model is capable to quantitative reproduce the dynamical behavior of the real system, but the actual simulated thermodynamic temperature has to be shifted by ≈ 20 K upward. In the following, as is our aim to compare the simulation results with the experiments, the reported MD temperatures are always shifted by such an amount.

We have studied a microcanonical (constant energy) system composed by 108 molecules (324 rings, 1944 Lennard Jones interaction sites) enclosed in a constant volume cubic box with periodic boundary conditions. To integrate the equations of motion we have treated each ring as a separate rigid body, identified by the position of its center of mass \bar{R}_i and by its orientation expressed in terms of quaternions \bar{q}_i [17]. The standard Verlet leapfrog algorithm [17] has been used to integrate the translational motion while, for the orientational part, a refined algorithm has been used [18]. The integration time-step is $\delta t = 2$ fs, which gives rise to an overall energy conservation better than 0.01 % of the kinetic energy.

We studied a wide temperature range spanning the liquid phase and reaching the glass region. In the different temperature runs the size of the cubic box has been chosen in order to keep the system at the coexistence curve experimental density [19,20]. At each temperature, after an equilibration run (15 ns long) we start the calculation of the molecular dynamics trajectory. It is worth to note that the system in the low temperature side of

the supercooled region and in the glassy phase is not equilibrated, as the diverging structural relaxation times do not allow simulation long enough to reach the equilibrium condition. Nevertheless, as we are interested to the high frequency properties, i.e. to those properties deriving from the intra-basin dynamics of the system, we think that it is not really important that the inter-basin dynamics was really equilibrated. Actually, also in the real experiments, whose outcome we are going to compare with the simulation, one investigates the glassy phase in similar non-equilibrium situation: the relaxation times in the glassy phase are very long, even in comparison with the experimental measuring times. During the MD evolution, lasting for $t_M=640$ ps, the configurations of the system are stored for subsequent analysis every 20 (50) time step for the runs at $T > (<)$ 280 K. All the calculations have been performed on a cluster of four α -CPU with a frequency of 500 MHz; every nanosecond of simulated dynamics needed approximately 24 hours of CPU-time.

From the stored configuration we calculate the dynamic structure factor as measured in an Inelastic X-ray Scattering (IXS) experiment [12,13]. The IXS technique measures the electron charge density fluctuation correlation function. As we consider the phenyl ring as a rigid body -i. e. we are not interested in the intra-ring vibrational dynamics that takes place at frequencies much higher than those investigated here- we can consider as fixed the phenyl ring charge distribution. Within this approximation, the scattering center can be considered as the ring center of mass, and the effect of the spatial distribution of the electron charge is summarized in a Q dependent phenyl ring form factor not affecting the frequency shape of $S(Q,\omega)$. Moreover, as we are not comparing neither the calculated and measured absolute scattering intensities nor their Q -dependence, we neglect hereafter the presence of such a form factor. Therefore, the appropriate dynamic structure factor [21] to be compared with the IXS experimental results is given by the power spectrum of the phenyl ring center number density fluctuation $\delta\rho_{\bar{Q}}(t)$:

$$\delta\rho_{\bar{Q}}(t) = \frac{1}{\sqrt{N}} \sum_j e^{i\bar{Q}\cdot\bar{R}_j(t)} \quad (1)$$

$$S(Q,\omega) = \frac{1}{t_M} \left| \int_0^{t_M} dt \delta\rho_{\bar{Q}}(t) e^{i\omega t} \right|^2. \quad (2)$$

In this equation t_M is the observation time for the variable $\delta\rho_{\bar{Q}}(t)$. The dynamic structure factors have been evaluated at the Q values allowed by periodic boundary condition of the simulation box: $\bar{Q} = 2\pi/L (n, m, l)$, with n, m, l integers and has been sampled at circular frequency between 0 and 22 ps^{-1} with a step of $\approx 0.075 \text{ ps}^{-1}$. The smallest accessible Q value is $\approx 1.8 \text{ nm}^{-1}$.

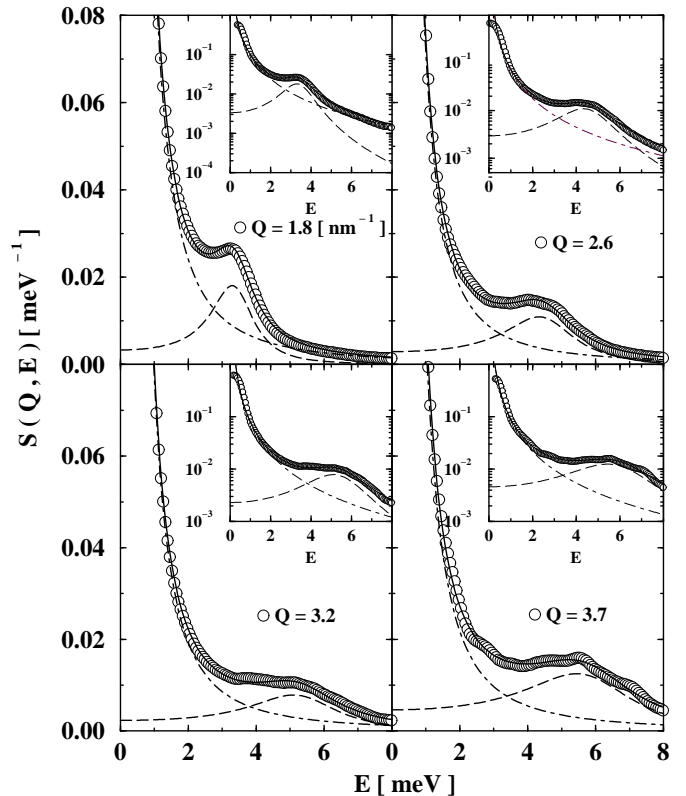


FIG. 1. Selected examples of the Q dependence of the $S(Q,\omega)$ calculated from the MD runs (open circles) at $T=50$ K and at the indicated Q values. The data are shown in linear and logarithmic scale, in the main figures and in the insets respectively. The full lines represent the fit of the data to Eq. (7), while the dashed (dot-dashed) lines is the individual elastic (inelastic) contributions to Eq. (7).

To increase the statistics, the $S(Q,\omega)$ at different Q values have been binned in channels 0.2 nm^{-1} wide, a value comparable to the experimental Q resolution. The frequency resolution, dictated by the time extension of the runs, is $\Delta\omega=0.15$ (0.75) ps^{-1} for $T > (<)$ 280 K. The choice of different frequency resolutions below and above 280 K is due to the fact that below this temperature the width of the central line (proportional to the inverse of the structural relaxation time τ_α) becomes so small that is no longer measurable. It is therefore preferable to relax the energy resolution in order to increase the statistics of the data. Above 280 K, the width of the central line is measurable, but a “good” energy resolution is needed; this procedure produces, obviously, data with much poorer statistics.

III. RESULTS

Selected $S(Q,\omega)$ [22] at $T=50$ K and at $Q=1.8, 2.6, 3.2$ and 3.7 nm^{-1} are reported in Fig. 1 (open circles).

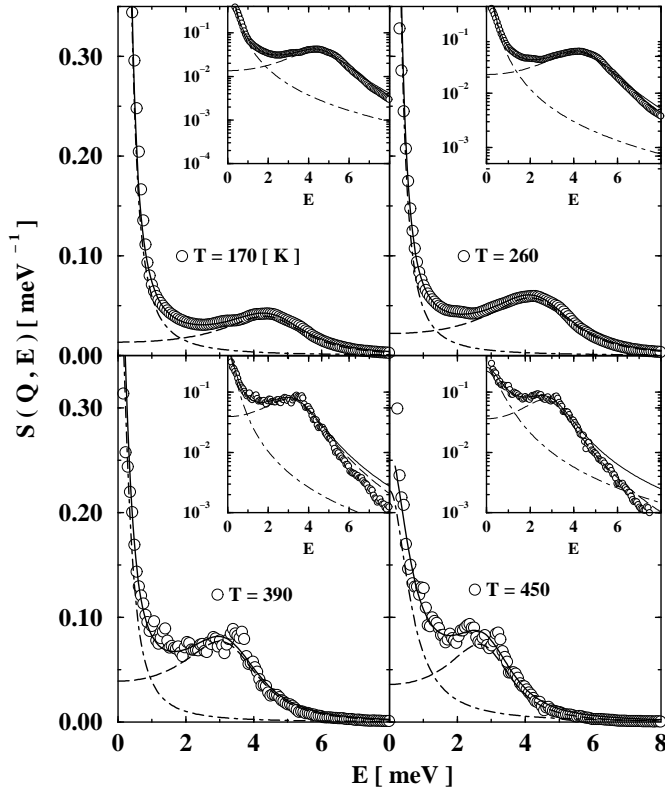


FIG. 2. Selected examples of the T dependence of the $S(Q, \omega)$ at the fixed Q value of 2.6 nm^{-1} . Similarly to Fig. 1 the data are shown in linear and logarithmic scale in the main figures and in the insets respectively. The full lines represent the fit of the data to Eq. (7), while the dashed (dot-dashed) lines is the individual elastic (inelastic) contributions to Eq. (7).

In all the figures, to be consistent with the experimental data, the $S(Q, \omega)$ have been reported as a function of the energy (E) measured in meV rather than as a function of the circular frequency ω . For completeness we recall that $\omega[\text{ps}^{-1}] \approx 1.61 E[\text{meV}]$. As the inelastic features appear as weak shoulder of an intense central peak, for each Q values the $S(Q, \omega)$ are shown both in linear (main figures) and in logarithmic (insets) intensity scale. We are interested in extracting the relevant parameters from the calculated $S(Q, \omega)$.

A formally exact way to treat these functions goes through the description of the density fluctuation correlation function $F(Q, t) = \langle \delta\rho_{\vec{Q}}(t)\delta\rho_{\vec{Q}}^*(0) \rangle$, i. e. the frequency Fourier transform of $S(Q, \omega)$ in term of a generalized Langevin equation [23]:

$$\ddot{F}(Q, t) + \omega_o^2 F(Q, t) + \int_0^t m(Q, t-t') \dot{F}(Q, t') dt = 0 \quad (3)$$

where $\omega_o^2 = k_B T Q^2 / M S(Q)$, $m(Q, t)$ is the "memory function" and $S(Q)$ is the static structure factor. This equation is "exact", but all the difficulties associated to the calculation of the $S(Q, \omega)$ have been transferred to the

determination of $m(Q, t)$. The advantage of this formulation stays in the fact that -independently from the choice of $m(Q, t)$ - the first two sum rules for $S(Q, \omega)$ are automatically satisfied:

$$\int d\omega S(Q, \omega) = F(Q, t=0) = S(Q) \quad (4)$$

$$\int d\omega \omega^2 S(Q, \omega) = -\ddot{F}(Q, t=0) = \frac{K_B T}{M} Q^2$$

By Fourier transform of Eq. (3), it is easy to show that:

$$S(Q, \omega) = \frac{\pi^{-1} S(Q) \omega_o^2 m'(Q, \omega)}{[\omega^2 - \omega_o^2 + \omega m''(Q, \omega)]^2 + [\omega m'(Q, \omega)]^2} \quad (5)$$

where $m'(Q, \omega)$ and $m''(Q, \omega)$ are the real and imaginary part of the time Fourier transform of the memory function. In the $\omega\tau_\alpha \gg 1$ limit, a limit that is valid in all the investigated temperature range [20], the memory function can be considered as the sum of two contribution: a constant -which reflects the α -process frozen on the time scale of the sound waves- plus a very fast decay at short time. The latter contribution to the memory function -often referred to as "microscopic" or "instantaneous"- is usually represented as a delta-function. Introducing the two constants representing the area of the "instantaneous" process and the long time limit of the memory function, $2\Gamma(Q)$ and $\Delta_\alpha^2(Q)$, the memory function is approximated by

$$m(Q, t) = 2\Gamma(Q)\delta(t) + \Delta_\alpha^2(Q) \quad (6)$$

and therefore, using Eq. (5), the $S(Q, \omega)$ reduces to:

$$S(Q, \omega) = S(Q) \times \left[f_Q \delta(\omega) + (1 - f_Q) \frac{1}{\pi} \frac{\Omega^2(Q) \Gamma(Q)}{(\omega^2 - \Omega^2(Q))^2 + \omega^2 \Gamma^2(Q)} \right] \quad (7)$$

where $\Omega(Q) = \sqrt{\Delta_\alpha^2(Q) - \omega_o^2}$ and $f_Q = 1 - \omega_o^2 / \Omega^2(Q)$. This expression is the sum of an elastic line (the frozen α process) and of an inelastic feature which is formally identical to a Damped Harmonic Oscillator (DHO) function; the central line accounts for a fraction f_Q -the Debye-waller or non-ergodicity factor- of the total intensity.

Recently it has been shown both via MD [24] and via IXS [25] that the "microscopic" contribution to the memory function cannot be represented by a delta-function. There are, indeed, clear indications that this "microscopic" part is responsible for a positive dispersion of the sound velocity in "harmonic" model glasses [24], and is responsible for the majority of the positive dispersion of the sound velocity in liquid lithium [25]. The simplest generalization of the delta function appearing in Eq. (6) considers a simple Debye-like "microscopic" contribution to the memory function:

$$m(Q, t) = \Delta_\mu^2(Q) e^{-t/\tau_\mu} + \Delta_\alpha^2(Q). \quad (8)$$

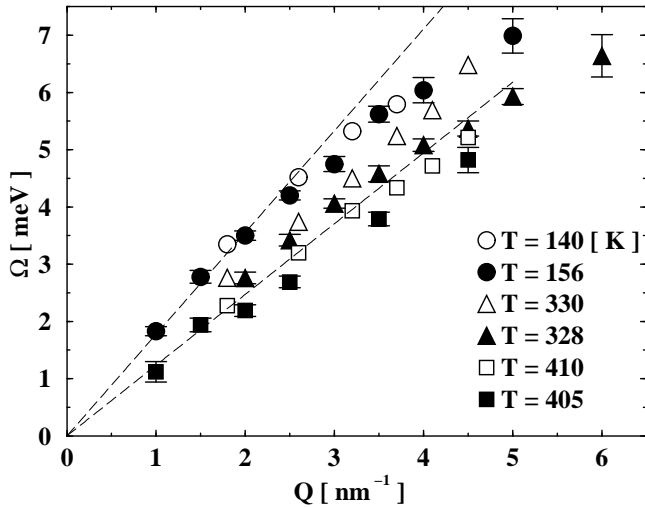


FIG. 3. Q dependence of the excitations frequency $\Omega(Q)$ at the indicated selected temperatures (open symbols for MD data and closed symbols for IXS data) as derived from the fit of the $S(Q, \omega)$ to Eq. (7). The dashed lines are guide to the eye.

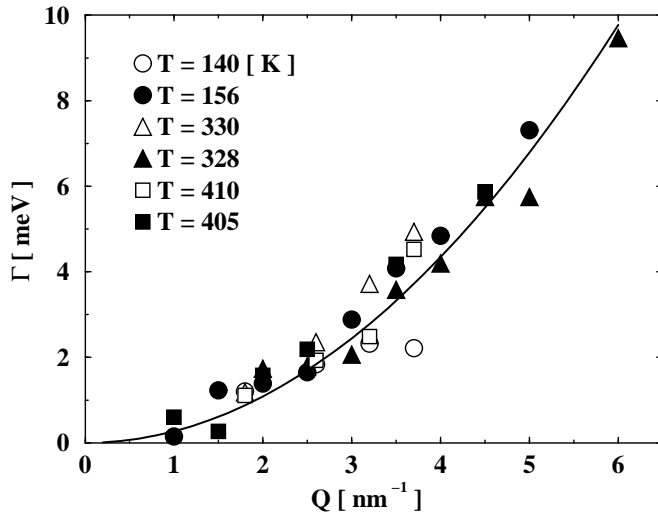


FIG. 4. Q dependence of the excitations broadening $\Gamma(Q)$ at the indicated selected temperatures (open symbols for MD data and closed symbols for IXS data) as derived from the fit of the $S(Q, \omega)$ to Eq. (7). The full line is a quadratic ($\Gamma(Q) = dQ^2$) fit to the whole set of data.

The quantity τ_μ entering in this equation is the characteristic time of the “microscopic” contribution to the memory function. Obviously, whenever $\Omega\tau_\mu \ll 1$, Eq. (8) produces for $S(Q, \omega)$ a DHO-like lineshape with $\Omega(Q) = \sqrt{\Delta_\alpha^2(Q) + \omega_0^2}$ and $\Gamma(Q) = \Delta_\mu^2(Q)\tau_\mu$.

In analyzing the IXS spectra of OTP, the author of Ref. [12] used the simplified DHO expression for the $S(Q, \omega)$ without noticing any systematic deviation of the experimental data from the fitting lineshape.

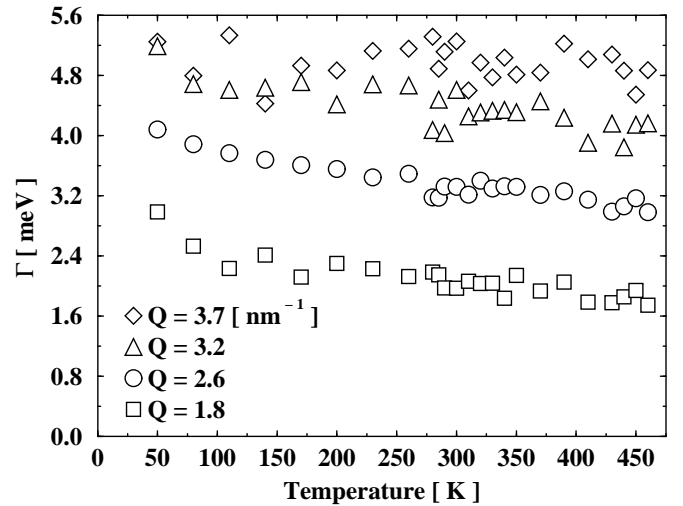


FIG. 5. T dependence of the excitations broadening $\Gamma(Q)$ at the indicated selected Q values as derived from the fit of the $S(Q, \omega)$ to Eq. (7).

Here, in order to better compare the MD results with the IXS one, we will follow the same procedure and analyze the calculated $S(Q, \omega)$ to the lineshape reported in Eq. (7). It is worth to note, however, that the MD data, less noisy and less affected by the resolution function than the experimental data, actually allows to establish that the $S(Q, \omega)$ obtained by the use of the memory function in Eq. (8) produces a better fit of the data. The fits to the MD $S(Q, \omega)$ using Eq. (7) has been made via the minimization of the standard χ^2 function, and the results are reported in Fig. 1 as full lines. The individual contributions (elastic and inelastic) are also shown (dashed and dot-dashed lines). The agreement between the MD data and the fitting function is satisfactory for all the investigated T and for all the investigated Q . An example of the T dependence of the $S(Q, \omega)$ at $Q = 2.6 \text{ nm}^{-1}$ is reported in Fig. 2, again in linear (main figure) and logarithmic (inset) scale and together with the best fit to a DHO lineshape.

The Q -dependences of the DHO parameters $\Omega(Q)$ and $\Gamma(Q)$ together with the experimental results of Refs. [12,13] at selected temperatures are reported in Figs. 3 and 4 respectively [26]. These figures confirms the experimental findings (see Fig. 1 in [12] and Fig. 2 in [13]) that: i) The excitations frequencies $\Omega(Q)$ show a clear Q dependence, which approach a linear behavior at small Q 's and bent down at increasing Q values; ii) The slope at small Q of $\Omega(Q)$ shows a marked T dependence together with its overall shape; iii) The parameters $\Gamma(Q)$ follow a Q^2 behavior; and iv) The temperature dependence of $\Gamma(Q)$ is much less pronounced than that of $\Omega(Q)$.

The latter T dependence is better emphasized in Fig. 5, where the parameter $\Gamma(Q)$ is reported -for the indicated selected Q values- at all the investigated temperatures.

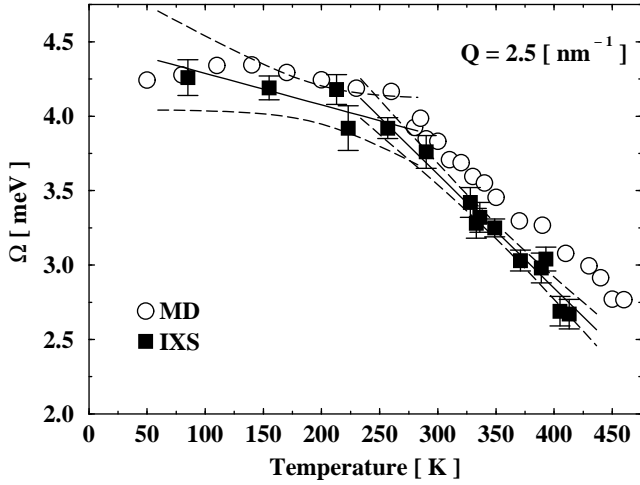


FIG. 6. T dependence of the excitations frequency $\Omega(Q)$ at $Q=2.6 \text{ nm}^{-1}$ (scaled at $Q=2.5 \text{ nm}^{-1}$ as explained in [27]) and as derived from the fit of the calculated $S(Q, \omega)$ to Eq. (7) (open circles). Also reported are the values of $\Omega(Q)$ at $Q=2.5 \text{ nm}^{-1}$ determined from the IXS experiment (full squares) [12]. The full lines are the best fit to the experimental points in the low- and high-temperature regions: they cross at the temperature T_x . The dashed lines indicate the limit of $\pm\sigma$ predictions band.

A decrease (line narrowing) of $\Gamma(Q)$ of about 20% is observed between the glassy phase at 50 K and the liquid phase (450 K). This decreasing behavior can be explained remembering that, in the $\Omega(Q)\tau_\mu \ll 1$ limit, the parameter $\Gamma(Q)$ is given by:

$$\Gamma(Q) = \Delta_\mu^2(Q)\tau_\mu = (\Omega_\infty^2(Q) - \Omega^2(Q))\tau_\mu \quad (9)$$

and considering that both $\Omega(Q)$ and $\Omega_\infty(Q)$ are linear in Q and proportional to the sound velocities appropriate to frequencies always much larger than $1/\tau_\alpha$ but respectively smaller and larger than $1/\tau_\mu$. The decrease of $\Gamma(Q)$ with increasing T reflects therefore the decrease of the sound velocities with increasing T . It is also important to point out that Eq. (9) gives also an explanation for the observed Q^2 behavior of $\Gamma(Q)$, when the reasonable hypotheses of a weak Q dependence of τ_μ and of the sound velocities are made. Overall the MD results reported in Figs. 2 - 5 are in agreement with the IXS experimental findings and give further support to the picture where propagating high frequency sound modes exist in glasses and liquids. These excitations are characterized (in the small Q limit) by a linear and a quadratic Q dependence of the excitations frequency and sound absorption coefficient respectively.

To be more quantitative, we report in Fig. 6 the comparison of the T dependence of the $\Omega(Q)$ parameter at fixed Q value of 2.5 nm^{-1} [27] as derived from the DM and IXS data. The two set of data are in satisfactory agreement.

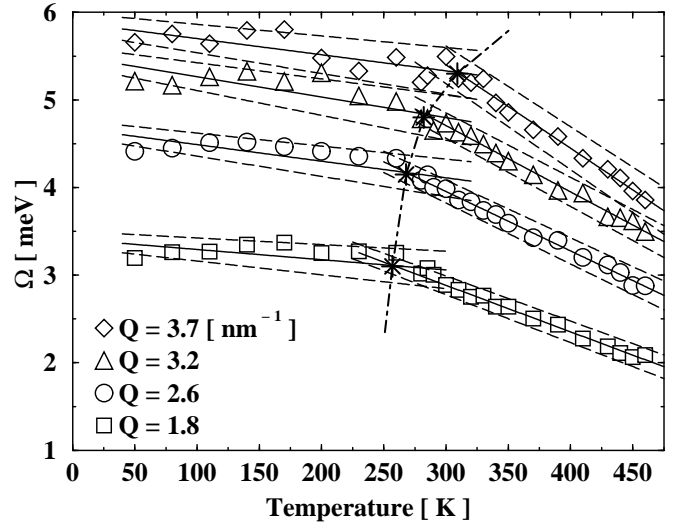


FIG. 7. T dependence of the excitations frequencies $\Omega(Q)$ at the indicated Q values derived from the fit of the calculated $S(Q, \omega)$ to Eq. (7) (open symbols). The full lines are the best fit to the points in the low- and high-temperature regions: they cross at the temperature $T_x(Q)$, indicated by stars. The dashed lines indicate the limit of $\pm\sigma$ predictions band: their lowest and highest T crossing are used to define the error bar for $T_x(Q)$. The dot-dashed line is a guide to the eye and connects the different discontinuity temperature.

The MD data lie slightly above the experimental ones, a feature that we ascribe to the non perfect tuning of the molecular potential model. It is important to underline that, similarly to the experimental data, also the MD derived $\Omega(Q = 2.5 \text{ nm}^{-1})$ show a discontinuity of slope at a temperature around T_g . A discontinuity that also in the MD data appears to be located at a temperature slightly above the calorimetric glass transition temperature. However, the single set of data at $Q = 2.5 \text{ nm}^{-1}$ is not conclusive. A more complete picture can be derived from the data reported in Fig. 7, where the T dependence of $\Omega(Q)$ is reported for four different Q values. Here one can clearly see that the temperature $T_x(Q)$ where is observed the slope discontinuity shows a well defined Q dependence, and seems to approach T_g decreasing Q . This observation, obviously, indicates that the shape of the dispersion relation $\Omega(Q)$ is modified by changing T . Therefore it is not possible to scale all the $\Omega(Q)$ vs. Q curves on top of each others by a factor, and it is important to study the $Q \rightarrow 0$ limit of these dispersion relations. This extrapolation is illustrated in Fig. 8 where, at four selected temperatures, the “apparent” sound velocity $c(Q) = \Omega(Q)/Q$ is reported vs. Q . A fit of these apparent velocities to a quadratic function, $c(Q) = c(Q = 0) + aQ^2$ is then performed (dashed lines in Fig. 8). The $Q = 0$ sound velocity, obtained by such an extrapolation are reported in Fig. 9, together with the similar quantity derived from the IXS data [13].

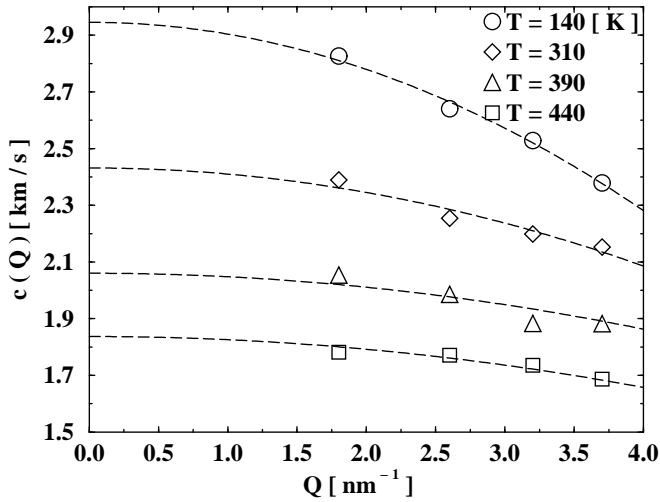


FIG. 8. The apparent sound velocities $c(Q) = \Omega(Q)/Q$ are reported as a function of Q at the four indicated temperatures. The dashed lines are the best fits of $c(Q)$ to a quadratic function, $c(Q) = c(Q=0) + aQ^2$, and are used to determine the $Q=0$ limit of the sound velocity.

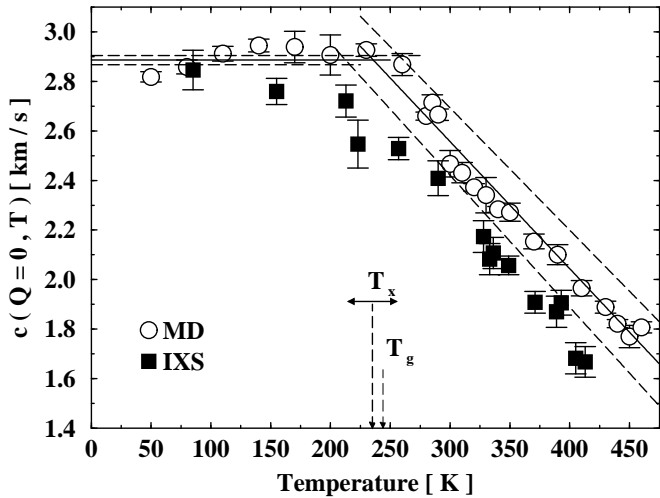


FIG. 9. T dependence of the sound velocity at $Q=0$ derived from the fits as in Fig. 8 (open circles). Also reported are the corresponding values determined from the IXS experiment (full squares) [13]. The full lines are the best fit to the MD points in the low- and high-temperature regions: they cross at the temperature $T_x(Q=0)$. The dashed lines indicate the limit of $\pm\sigma$ predictions band.

Again we found a good agreement between simulated and experimental data, and again the two sets of data show a slope discontinuity at a comparable temperature, that now *coincide within the statistic uncertainties* with T_g .

The overall picture is summarized in Fig. 10, where the discontinuity temperature $T_x(Q)$ is reported as a function of Q . Despite the large statistical error bars, it is evident that T_x has a marked Q dependence and, in particular, it is clear that it extrapolates to a temperature compatible with T_g as Q goes to zero.

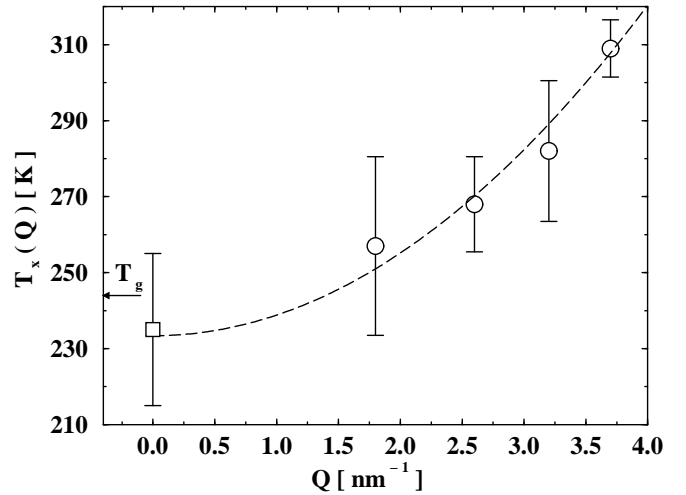


FIG. 10. Q dependence of the discontinuity temperature $T_x(Q)$ derived from Fig. 7 (open circles) and from Fig. 9 (open square). The error bars are determined by the crossing of the $\pm\sigma$ prediction bands. The dashed line is a guide to the eye. The horizontal arrow indicate the calorimetric glass transition temperature.

This result can be interpreted in the framework of the current understanding of the dynamics of supercooled liquids. Numerous MD simulations study [8–10] have recently pointed out the validity of the description of the supercooled liquid state in terms of the formalism initially introduced by Stillinger and Weber [11]: the point that represent the system in the $3N$ configurational space moves, in this space, performing a “fast” vibrational dynamics around a given minima of the potential energy hyper-surface and occasionally -with a rate dictated by the structural relaxation time τ_α - perform jumps between basins pertaining to different minima [8]. This “naive” description acquires more physical meaning with the demonstration [28–31] that the two dynamical regimes are almost decoupled, to the extent that the aging processes in glasses can be quantitatively described supposing that the two subsystem are equilibrated at different temperatures. In this framework, it has been demonstrated [30,31] that, approaching the glass transition temperature, the representative point visits minima of lower and lower potential energy, and exist a strict relation between the temperature and the energy of the minima visited. As demonstrated in the case of Binary Mixture Lennard Jones (BMLJ) [30,31] systems, different minima have also -on average- different metric properties, as for example the curvatures at the minimum point and therefore the distribution of vibrational eigenfrequencies.

Our findings on the Q -dependence of the discontinuity temperature T_x can be interpreted within this framework. Similarly to Lennard-Jones systems, also in the case of OTP we found that the modification of the eigenfrequencies (local curvatures) does not follow a simple scaling, but there is a deformation of the shape of the density of vibrational states in changing the energy of

the minima. In particular, upon cooling, i. e. on going to lower and lower energy minima, the highest curvatures (highest frequency, highest Q) reach their limiting values (those pertaining to the “ideal” glassy minima) before than the lowest curvatures do.

IV. CONCLUSIONS

In this paper we have reported results about Molecular Dynamics calculation of the high frequency dynamics on the flexible molecule model of orthoterphenyl introduced in Ref. [14]. The collective dynamics structure factor has been determined in a wide exchanged momentum and temperature range and has been compared to the its experimental measurements performed by means of Inelastic X-ray Scattering [12,13,20]. The relevant parameters that describe the overall spectral shape have been determined using the same model already utilized in the analysis of the experimental data, i. e. the sum of an elastic contribution and a DHO lineshape. The resulting parameters $\Omega(Q)$ and $\Gamma(Q)$ -the position and broadening of the inelastic peaks respectively- are in good agreement with the corresponding experimentally determined quantities. Moreover the present simulation confirms the existence in liquids and glasses of propagating sound waves at high frequency and shows that: i) The excitation frequencies $\Omega(Q)$ show a clear Q dependence, which approach a linear behaviour at small Q 's and bent down at increasing Q values; ii) The slope at small Q of $\Omega(Q)$ shows a marked T dependence together with its overall shape; iii) The parameters $\Gamma(Q)$ follows a Q^2 behaviour; and iv) the temperature dependence of the high frequency sound attenuation coefficient, related to $\Gamma(Q)$, is only weakly dependent on T . The latter result further support the findings of a sound attenuation mechanism not related to anharmonicity [4].

More important, we find that -similarly to the experimental findings of Ref. [12]- the temperature dependence of the excitation frequency at constant Q value shows a slope discontinuity at a temperature T_x close to, but definitively larger than, the calorimetric glass transition temperature. By extending the Q values where this analysis is performed, we found clear evidence of the Q -dependence of T_x . In particular, we find that $T_x(Q)$ approaches T_g in the $Q \rightarrow 0$ limit. The existence of a T dependence of the $S(Q, \omega)$ peaks position can be explained by the results of recent MD studies of Lennard-Jones systems where the T -dependence of the curvatures of the PES at the inherent structures were clearly evidenced. The findings of a Q -dependent transition temperature is an indication of the fact that the density of vibrational states does not change according to a frequency scaling law. Rather it is deformed in such a way that the highest frequency reach the limiting value pertaining to the “ideal” glassy minimum before than the lowest frequency.

Finally, our results indicate a possible *experimental* way to validate or disprove the PES-based interpretation of the glass transition phenomenology.

ACKNOWLEDGEMENTS

We thanks R. Di Leonardo and T. Scopigno for intensive discussions during the data analysis.

-
- [1] C. A. Angell, *Science* **267**, 1924 (1995).
 - [2] C. A. Angell, K. L. Ngai, G. B. McKenna, P. F. McMillan, and S. W. Martin, *J. Appl. Phys.* **88**, 3113 (2000).
 - [3] F. Sette, M. Krisch, C. Masciovecchio, G. Ruocco and G. Monaco, *Science* **280**, 1550 (1998).
 - [4] G. Ruocco, F. Sette, R. Di Leonardo, D. Fioretto, M. Lorentzen, M. Krisch, C. Masciovecchio, G. Monaco, F. Pignon, and T. Scopigno., *Phys. Rev. Lett.* **83**, 5583 (1999).
 - [5] M. Mézard and G. Parisi, *Phys. Rev. Lett.* **82**, 747 (1999); M. Mézard and G. Parisi, *J. Phys.: Condens. Matter* **12**, 6655 (2000).
 - [6] W. Götze, in *Liquids, Freezing and the Glass Transition*, edited by J. P. Hansen, D. Levesque and J. Zinn-Justin (North-Holland, Amsterdam, 1991); W. Götze and L. Sjörger, *Rep. Prog. Phys.* **55**, 241 (1992); W. Götze, *J. Phys.: Condensed Matter*, **11**, A1 (1999).
 - [7] R. Schilling, in *Disorder Effects on Relaxational Processes* edited by A. Richert and A. Blumen (Springer Verlag, 1994); W. Kob, in *Experimental and Theoretical Approaches to Supercooled Liquids: Advances and Novel Applications* edited by J. Fourkas *et al.* (ACS Books, Washington, 1997).
 - [8] F. Sciortino, W. Kob, and P. Tartaglia, *Phys. Rev. Lett.* **83**, 3214 (1999).
 - [9] L. Angelani, R. Di Leonardo, G. Ruocco, A. Scala, and F. Sciortino, *Phys. Rev. Lett.* **85**, 5356 (2000); E. La Nave, A. Scala, F. W. Starr, F. Sciortino, and H. E. Stanley, *Phys. Rev. Lett.* **84**, 4605 (2000); L. Angelani, R. Di Leonardo, G. Parisi, and G. Ruocco, Preprint condmat/0011519.
 - [10] A. Heuer, *Phys. Rev. Lett.* **78**, 4051 (1997); S. Buechner and A. Heuer, *Phys. Rev. E* **60**, 6507 (1999); S. Sastry, P. G. Debenedetti, and F. H. Stillinger, *Nature* **393**, 554 (1998); B. Coluzzi, P. Verrocchio, and G. Parisi, *Phys. Rev. Lett.* **84**, 306 (2000); T. B. Schröder, S. Sastry, J. Dyre, and S. C. Glotzer, *J. Chem. Phys.* **112**, 9834 (2000); S. Sastry, *Nature* **409**, 164 (2001).
 - [11] F. H. Stillinger and T. A. Weber, *Phys. Rev. A* **25**, 978 (1982); *Science* **225**, 983 (1984); F. H. Stillinger, *Science* **267**, 1935 (1995).
 - [12] C. Masciovecchio, G. Monaco, F. Sette, A. Cunsolo, M. Krish, A. Mermet, M. Solwisch, and R. Verbeni, *Phys. Rev. Lett.* **80**, 544 (1998).
 - [13] G. Monaco, C. Masciovecchio, G. Ruocco, and F. Sette, *Phys. Rev. Lett.* **80**, 2161 (1998).

- [14] S. Mossa, R. Di Leonardo, G. Ruocco, and M. Sampoli, Phys. Rev. **E 62**, 612 (2000).
- [15] S. Mossa, G. Ruocco, and M. Sampoli, Preprint cond-mat/0012474.
- [16] S. Mossa, Ph. D. thesis, Università di L'Aquila, 1998 (unpublished).
- [17] M. P. Allen and D. J. Tildesley, *Computer Simulation of Liquids* (Clarendon Press, Oxford, 1989).
- [18] G. Ruocco and M. Sampoli, Mol. Phys. **82**, 875 (1994).
- [19] J. N. Andrews, and A. R. Ubbelohde, Proc. Roy. Soc. A **228**, 435 (1955); R. J. Greet, and D. Turnbull, J. Chem. Phys. **46**, 1243 (1967); G. Friz, G. Kuhlbörsch, R. Nehren, and F. Reiter, Atom Kerenergie **13**, 25 (1968); W. H. Hedley, M. V. Milnes, and W. H. Yanko, J. Chem. Eng. Data **15**, 122 (1970); M. Naoki, and S. Koeda, J. Phys. Chem. **93**, 948 (1989).
- [20] G. Monaco, Ph.D. thesis, Università di L'Aquila, 1997 (unpublished).
- [21] J. P. Hansen and J. R. Mc Donald, *Theory of Simple Liquids* (Academic Press Limited, London, 1986).
- [22] It is worth noting that the following general discussion of the models for the dynamic structure factor will be given in terms of the frequency ω , at variance with all the available experimental data which express the energy in meV. In view of the comparison between MD and the experimental results all the data points in the pictures are expressed in meV.
- [23] U. Balucani and M. Zoppi, *Dynamics of the Liquid State*, (Clarendon Press, Oxford, 1994).
- [24] G. Ruocco, F. Sette, R. Di Leonardo, G. Monaco, M. Sampoli, T. Scopigno, and G. Viliani, Phys. Rev. Lett. **84**, 5788 (2000).
- [25] T. Scopigno, U. Balucani, G. Ruocco, and F. Sette., J. of Phys. C **12**, 8009 (2000); T. Scopigno, U. Balucani, G. Ruocco, and F. Sette., Phys. Rev. Lett. **85**, 4076 (2000).
- [26] It is worth noting that sometimes in the literature in Eq. (6) appears the term Γ instead of 2Γ ; this is actually the case of Refs. [3,4]. In order to preserve the consistency with Eq. (6) we then show both the actual experimental and MD values for Γ multiplied by 2.
- [27] The experimental data were collected at $Q=2.5 \text{ nm}^{-1}$, while the present MD data are calculated at $Q=2.6 \text{ nm}^{-1}$. To account for the small differences in the Q values -and therefore in the Ω values- we have scaled the MD calculated $\Omega(Q)$ by the factor 2.5/2.6, appropriate for a linear Q dependencies of the excitation frequency.
- [28] G. Parisi, Phys. Rev. Lett. **79**, 3660 (1997); J. L. Barrat, and W. Kob, Europhys. Lett. **46**, 637 (1999).
- [29] R. Di Leonardo, L. Angelani, G. Parisi, and G. Ruocco, Phys. Rev. Lett. **84**, 6054 (2000).
- [30] W. Kob, F. Sciortino, and P. Tartaglia, Europhys. Lett. **49**, 590 (2000).
- [31] F. Sciortino, and P. Tartaglia, Preprint cond-mat/0007208.